*remote sensing*

MDPI

*Article*

# Shortwave Radiation Affected by Agricultural Practices

**Jerzy Cierniewski [1,*], Jakub Ceglarek [1], Arnon Karnieli [2], Eyal Ben-Dor [3], Sławomir Królewicz [1] and Cezary Kaźmierowski [1]**

[1] Department of Soil Science and Remote Sensing of Soils, Adam Mickiewicz University in Poznań, Bogumiła Krygowskiego 10, 61-680 Poznań, Poland; jakub.ceglarek@amu.edu.pl (J.C.); skrol@amu.edu.pl (S.K.); cezark@amu.edu.pl (C.K.)

[2] Remote Sensing Laboratory, Jacob Blaustein Institutes for Desert Research, Ben Gurion, University of the Negev, Sede Boker Campus, Sede-Boker 84990, Israel; karnieli@bgu.ac.il

[3] The Remote Sensing Laboratory, Department of Geography, School of Earth Science Faculty of Exact Science, Tel Aviv University, Tel Aviv 69989, Israel; bendor@post.tau.ac.il

* Correspondence: ciernje@amu.edu.pl

Received: 28 November 2017; Accepted: 6 March 2018; Published: 9 March 2018

**Abstract:** The albedo of bare soil depends on its organic matter, iron oxide, carbonate contents, and reflectance geometry, features considered stable over time, and also depends on salinity, moisture and roughness, which change dynamically due to agricultural practices. This paper deals with the quantitative estimation of the amount of shortwave radiation that could be reflected by air-dried bare soils in clear-sky conditions within arable lands in Israel throughout the year, assuming that they were shaped by a plough, a disk harrow, or a smoothing harrow. An area of bare soils was extracted from Landsat 8 images, within the contours of arable lands. The radiation reflected from the bare soils was calculated by equations predicting variations in their half-diurnal albedo as the solar zenith angle function. Accordingly, laboratory reflectance data of Israeli soil samples were used. The results clearly showed annual variation in the amount of short-wave radiation reflected from all bare soils within arable lands. The minimum radiation occurred in the winter, between the 1st and 70th day of the year (DOY), and the maximum was identified in the summer between 200th and 250th DOY. This could reach about 3–5 PJ/day and 16–23 PJ/day, respectively.

**Keywords:** bare soil albedo; surface roughness; narrow to broadband albedo conversion; spectral reflectance

## 1. Introduction

The broadband albedo of bare soils depends on their brightness, which is affected mainly by the soil's content of organic matter, iron oxides, and carbonates and also by their reflectance geometry (slope aspect and the sun angle). These properties are considered to be stable with time or simply corrected, in contrast to soil surface roughness, salinity and moisture content, which change dynamically, especially due to agricultural practices in arable lands. The range of albedo (on a scale of 0–1) of dark-coloured, wet, and rough soils, is about 0.05–0.15, while that of light-coloured, dry, and smooth ones is usually 0.35–0.4 [1,2]. The increasing share of crop cover reduces the albedo of fields with light-colour soils, and increases the albedo of fields with dark-coloured soils [3]. Soil surfaces that do not have a shallow groundwater table beneath become dry quickly after rain events, achieving an air-dry moisture state and increasing their reflectance. Baumgardner et al. [4] and Cipra et al. [5] state that soil crusts are formed as a result of the repeated wetting and drying of soil surfaces, reducing soil roughness. Goldshleger et al. [6] demonstrated that raindrop energy is also responsible for increasing albedo by a segregation process, where fine particles move to the upper

soil layer and reflect more photons back to the sensor. A soil surface with large irregular aggregates has a lower spectral reflectance than the same soil with more spherical and smaller aggregates [7]. Matthias et al. [8] reported that the ploughing of soils decreased their reflectance by about 25%.

The albedo of soil affects the energy transfer between soil, vegetation and the atmosphere. This physical quantity can be used as input data in the modelling of global climate [9,10]. The use of agricultural cultivation tools to smooth soils decreases the amount of shortwave radiation absorbed by soil surfaces relative to the amount absorbed by soil, which is the same but has been shaped by a plough, and hence leads to a reduction in the temperature of those smoother surfaces, as lower emission of long-wave radiation occurs [11].

As with other land surfaces of the Earth, the albedo of soils varies during the day with the changing solar zenith angle ($\theta_s$). The albedo reaches its minimum at the local noon [12–15] and approaches one at the lowest position of the sun, when the sun rises and sets. The higher the diffuse light ratio, the smaller the impact of $\theta_s$ on the albedo. Cierniewski et al. [16] analysed the diurnal albedo variations of soils to find that soil roughness affected not only the overall level of those variations, but also that the intensity of its increase from $\theta_s$ at the local noon, to about 75°–80°. Surfaces of rough and deep ploughed soils showed almost no rise in albedo values at $\theta_s$ lower than 75°, while the same soil, but smoothed, exhibited a gradual albedo increase at these angles. Knowledge of the variation in albedo of soils seems especially important in light of statements that global climate models require an albedo accuracy of better than ±2% [17]. With the intention to, as precisely as possible, model processes associated with the flow of radiation between the Earth's surface and the atmosphere over longer periods of several days, a month, a season or a year, average diurnal albedo values appear to be more useful than instantaneous values [18–20]. Cierniewski et al. [21] used the average diurnal albedo values of soils within arable lands in Poland (various over the course of the year) to quantify the annual dynamics of shortwave radiation reflected from them under a clear sky, as a consequence of the smoothing of previously ploughed and harrowed soils when their surfaces were air-dry. This quantification, using data on the content of soil organic carbon and carbonates stored in soil databases, were carried out as part of the project entitled "Effects of tillage smoothing of soils on the increase in the amount of the shortwave radiation reflected from arable lands on a global scale throughout the year" (no. 2014/13/B/ST10/02111). The issue was considered in simplified situations when radiation could reach its highest values, that is, in clear-sky conditions and when the soil surfaces were air-dry.

The goal of the current paper is to estimate the highest possible amount of shortwave radiation that could be reflected from bare soils within arable lands in Israel throughout the year, depending on the roughness of the soil surfaces caused by the use of selected agricultural tools. As in the aforementioned paper referring to the arable land in Poland, it was assumed that the highest shortwave radiation levels reflected from the bare arable soils occur during clear-sky conditions and when their surfaces are air-dry. The estimation is based on their average diurnal albedo values, calculated from soil reflectance spectra, which is also stored in soil databases. That these soils belong to specific soil units having different spectral reflectance, was taken into account.

## 2. Materials and Methods

### *2.1. Study Area*

Three Landsat 8 scenes, based on the WRS-2 scheme (Worldwide Reference System version 2 global notation used in cataloguing Landsat data) that cover arable land in Israel, were selected as follows: 174/37, 174/38, and 174/39 (Figure 1). These scenes are derived from a continuously recorded image strip. The data were Level-1 Standard Data Products images recorded from the beginning of this satellite mission to December 2015 with less than 10% cloud cover and were obtained from the United States Geological Survey (USGS) using the EarthExplorer application (http://earthexplorer.usgs.gov). A total of 90 scenes (from 30 dates) were used for extraction of bare soil areas within the arable lands.

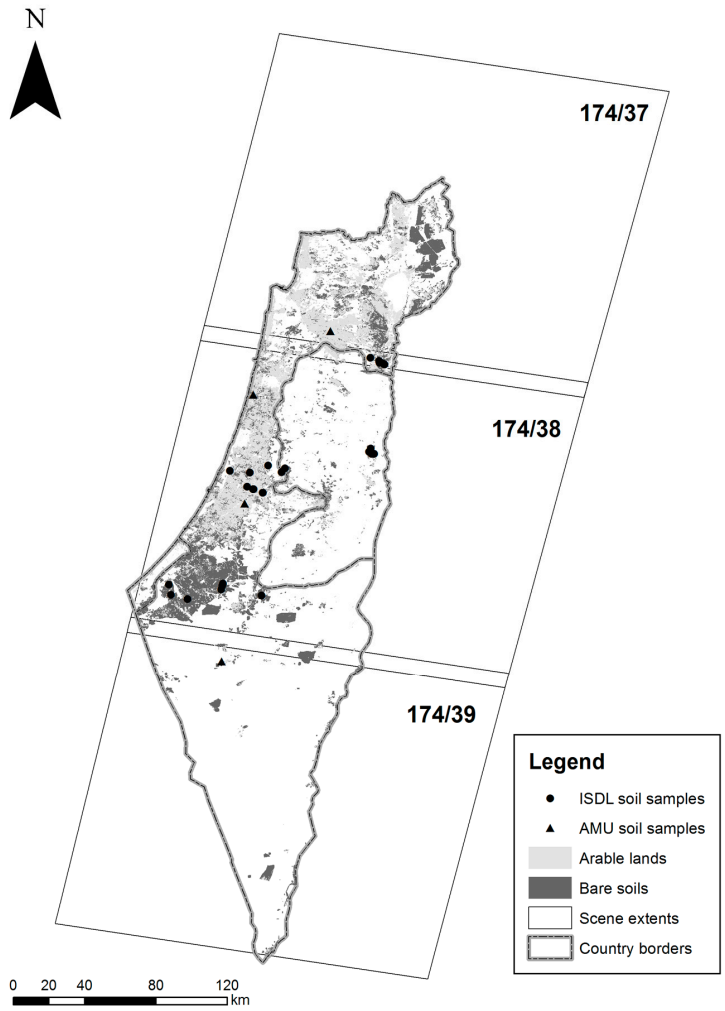


**Figure 1.** Location of soil samples obtained from the Israeli Soil Database Library (ISDL) and analyzed at Adam Mickiewicz University (AMU) based on bare soil areas extracted from the Landsat 8 images recorded on 9 September 2015, within arable land contours in Israel.

### *2.2. Extracting Bare Soil Areas*

Each of the optical image data corresponding to the three scenes recorded near the same time was mosaicked into a single integrated image. Next, they were radiometrically calibrated to the top-of-the-atmosphere reflectance (TOA) using metadata, and normalized from different illumination conditions by dividing TOA with the cosine of the solar zenith angle. Then, the extents of haze were estimated, clouds and shadows were masked out, atmosphere path radiance was corrected, and the ground reflectance was calculated assuming flat terrain. The listed processing operations were carried out using the PCI Geomatica software package with the implemented Atmospheric/Topographic Correction (ATCOR) algorithm [22]. The reflectance data of the five Operational Land Imager (OLI) bands of the integrated images were used to extract soil areas not covered by plants. These soils were identified as bare if their reflectance (RB) in the bands (B) 3–7 fulfilled the following conditions: $R_3 < R_4 < R_5 < R_6$, $R_6 > R_7$, and $R_6 – R_5 < 1$. This set of conditions was created on the basis of the spectra shape of main soil units occurring in Israel. The classification of bare soils has been limited to the extent of the arable land category that was located using the OpenStreetMap data, updated on the 3rd of September 2014. This limitation allowed simplifying the classification problem to only distinguishing between vegetation and bare soils. The effectiveness of the classification was validated according to the adopted criteria, by comparing its results with visual interpretation for 5% of the arable lands for

each of selected dates including winter, spring, summer, and autumn. The visual interpretation was performed on the color composition images in the RGB model, obtained by the combination of spectral bands $R_5$, $R_4$, $R_3$ (color-infrared), $R_7$, $R_4$, $R_3$, and $R_4$, $R_3$, $R_2$ (natural colors).

The results of the bare soil identification, performed for each integrated image, were presented in the form of binary maps with the spatial resolution of 30 m. Soil units on a digital soil map [23] originally classified according to the Israeli nomenclature system, were converted to the U.S. Soil Taxonomy system [24] and superimposed on contours of the extracted bare soils from the images at a given date. This allowed the bare soil areas of the soil units within arable lands of Israel to be measured for the particular days when the Lansdat scenes were recorded. All processing steps of the images and bare soil area statistics were done with scripts written in SML language—the programming environment included in the TNTmips software package.

### 2.3. Spectral Properties of Soil

Following the previous stages, each of the soil units was described in terms of the spectral reflectance properties of the soil samples that were located in its contours, as obtained from the Israeli Soils Library (https://www.tau.ac.il/rslweb/slis.html). To find a bare soil spectrum that could be representative of Israel's soils, the spectra of all the soil map units were weighted by their area share. The averaged data were used to calculate the half-diurnal albedo variation of all the bare arable soils in Israel. Their overall soil albedo level ($\alpha$) at a given roughness condition under $\theta_s = 45^\circ$ ($\alpha_{45}$ ) was calculated as [25]:

$$\alpha_{45} = 0.454 - 0.112T_{3D} + 6952.66x_{474} - 13108.37x_{705} + 12470.20x_{952} - 11597x_{1650}, \quad (1)$$

where $T_{3D}$ is the roughness index defined as the ratio of the real surface area within its basic unit to its flat horizontal area [26], and $x_l$ is diffuse reflectance data transformed to their second derivative for specified wavelength (l): 474, 705, 952, and 1650 nm. Meanwhile, their $\alpha$ under $0^\circ < \theta_s > 75^\circ$ ($a_{\theta_s}$) was calculated as:

$$a_{\theta_s} = \theta_{45}[1 + s_a(\theta_s - 45)], \quad (2)$$

where $s_a$ expresses the slope of the $a$ increases in this $\theta_s$ range:

$$s_a = 0.0008 + 0.00108T_{3D}^{-20.75}, \quad (3)$$

The half-diurnal $a$ variation of the soil units, relative to $\theta_s$, taking into account their roughness, was expressed in the full $\theta_s$ range up to 90° by the formula:

$$a_{\theta_s} = \frac{a + c\theta_s^{0.5}}{1 + b\theta_s^{0.5}}, \quad (4)$$

where $a$, $b$, and $c$ are fitting parameters. This equation was individually fitted to the soil units with roughness created by a plough (Pd), a disk harrow (Hd), and smoothing harrow (Hs) using TableCurve 2Dv5.01 (SYSTAT Software Inc., San Jose, CA, USA). Their roughness was described by $T_{3D}$ values as follows: 1.5, 1.15, and 1.05 for Pd, Hd, and Hs, respectively, based on a previous paper by Cierniewski et al. [20]. The correctness of the $a_{\theta_s}$ distributions, predicted by the Equations (1)–(4), was evaluated by the root mean square error (RMSE), using the generated data and their equivalents measured directly in the field at $\theta_s$ from 15° to 75°, in 15° increments.

### 2.4. Modeling of Albedo Using Soil Spectra

Then after, the weighted average $\alpha_{\theta s}$ distribution representative for the whole bare soils area within arable lands in Israel was expressed in relation to time, replacing the $\theta_s$ by solar local time. It became possible to predict the average values of the diurnal albedo of the soils ($\alpha_d$) formed by a Pd, an Hd, and an Hs within arable lands for all days of a year. Finally, multiplying $\alpha_d$ values by the total

amount of shortwave radiation coming to the soils on a given day (calculated using the formulas provided by Allen et al. [27]), the amount of shortwave radiation reflected from one square kilometer of the averaged bare soils formed by each of the above tools was predicted.

## 3. Results

### 3.1. Soil Units in the Study Area

Arable land in Israel occupied 3975 km$^2$ in 2014, representing 19% of the country land area (www.openstreetmap.org). The areas of bare soils within the contours of the arable lands were extracted from 7, 11, and 12 integrated images of Landsat 8 recorded in 2013, 2014, and 2015, respectively. Eleven soil units corresponding to the great group category of the U.S. Soil Taxonomy System were identified as not being covered by vegetation within the arable soils in Israel at the time of the overpasses. These units were described in terms of the soil properties of 28 soil samples obtained from the Israeli Soils Library, located within their contours on the digital soil map, and three samples taken in places where $\alpha_{\theta s}$ was directly measured in the field (Table 1). Figure 1 shows the location of the 28+3 samples. The great groups Haploxeralfs and Rhodoxeralfs, belonging to the Alfisols order, dominate among them, occupying on average (across 30 analyzed days) almost 29% of the total area of the bare soils within the arable lands (Table 1). The great groups Torrifluvents, Xerofluvents, Torriothents, and Xerothents, representing the Entisols order, occupied about 20% of the area, as did the Haploxerolls unit belonging to the Mollisols order. The Haploxererts unit, belonging to the Vertisols order, covered slightly less, at 19% of the area. The great groups Calciorthids and Haplorghids, belonging to the Aridisols order, occupied only 1% of the area.

**Table 1.** Properties of the studied soils, classified according to SSS (2014). * the soils for which the half-diurnal albedo variations were also measured directly in the field.

| Order | Suborder | Great Soil Group | ISDL and AMU Symbol | Texture by USDA | Munsell Dry Color | SOC (%) |
|---|---|---|---|---|---|---|
| Alfisols | Xeralfs | Rhodoxeralfs | E7 | SCL | 5YR6/6 | 0.39 |
| | | Rhodoxeralfs | E8 | LFS | 5YR7/8 | 0.08 |
| | | Rhodoxeralfs | NA1 * | LFS | 5YR4/6 | 0.54 |
| | | Haploxeralfs | S4 | LFS | 7.5YR7/4 | 0.58 |
| | | Haploxeralfs | S6 | SL | 10YR6/4 | 0.83 |
| | | Haploxeralfs | K2 * | L | 10YR7/4 | 0.86 |
| Aridosols | Agrids | Calciorthids | K3 | CL | 10YR5/2 | 1.87 |
| | | Calciorthids | K4 | CL | 10YR6/2 | 2.01 |
| | | Calciorthids | K5 | CL | 10YR6/1 | 1.65 |
| | | Calciorthids | K6 | SCL | 10YR6/1 | 1.70 |
| | | Calciorthids | K7 | CL | 10YR6/2 | 1.59 |
| | | Haplargids | H8 | CL | 7.5YR6/8 | 1.31 |
| | | Haplargids | H10 | C | 7.5YR7/4 | 1.02 |
| | | Haplargids | H11 | SL | 7.5YR7/4 | 0.77 |
| Entisols | Fluvents | Torrifluvents | J1 | C | 7.5YR6/4 | 1.40 |
| | | Torrifluvents | J2 | SIC | 7.5YR4/4 | 2.63 |
| | | Xerofluvents | S5 | LFS | 10YR7/3 | 0.61 |
| | | Xerofluvents | S15 | SCL | 10YR6/4 | 0.65 |
| | Orthents | Torriorthents | S9 | SL | 10YR7/4 | 0.78 |
| | | Torriorthents | S10 | SL | 10YR8/4 | 0.84 |
| | | Torriorthents | S11 | SL | 7.5YR8/3 | 0.60 |
| | | Xerorthents | C2 | SL | 10YR8/3 | 0.59 |
| | | Xerorthents | C3 | SCL | 7.5YR7/3 | 0.86 |
| | | Xerorthents | C5 | C | 10YR8/2 | 1.55 |
| | | Xerorthents | RM5 * | SL | 10YR7/4 | 0.66 |
| Inceptisols | Ochrepts | Xerochrepts | A4 | C | 7.5YR4/6 | 3.28 |
| | | Xerochrepts | A5 | C | 5YR5/6 | 1.46 |
| Mollisols | Xerolls | Haploxerolls | B1 | CL | 7.5YR6/3 | 2.85 |
| | | Haploxerolls | C4 | SC | 7.5YR5/4 | 1.11 |
| Vertisols | Xererts | Haploxererts | H4 | CL | 7.5YR6/2 | 2.19 |
| | | Haploxererts | H1 | CL | 10YR6/3 | 1.61 |
| | | Haploxererts | H2 | C | 10YR5/2 | 3.10 |

It was found that the acreages of the majority of the aforementioned great group units did not differ from their average values obtained from the 30 satellite observations by more than by 20% (Figure 2). Only the Calciorthids, Haplargids, Xerothents, and Xerofluvents, which occupied the smallest areas covering only a few pixels of the interpreted images, showed larger deviations in relation to their averaged areas, exceeding even 200%, 150%, 100% and 75%, respectively, in April 2014.

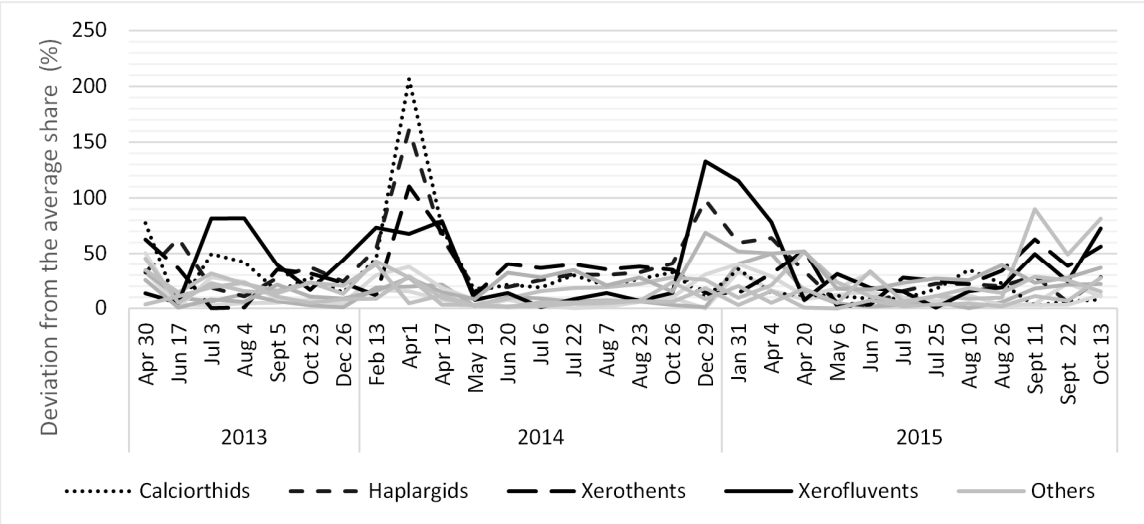


**Figure 2.** Deviation from the average share of the soil unit area not covered by vegetation within arable lands in Israel, extracted from 30 Landsat mosaicked images.

### *3.2. Spectral Properties of Soil*

All of the above-mentioned soil units have also been described in terms of reflectance spectra measured in a laboratory, corresponding to the 28+3 soil samples (Figure 3). Most of the spectra of the bright soil orders, (Alfisols and Entisols) which have a color value higher than five, were developed from soil materials of different texture. In addition, the soil organic carbon (SOC) content in these soils was lower than 1.5%. These soils showed the highest reflectance, with a characteristic convexity in the visible spectral region (yellow and longer) (Table 1). Meanwhile, the Caliorthids great group, belonging to the Aridisols, had a clearly concave spectra in the visible and the near infrared range. Most of the dark soil orders, the Vertisols, Inceptisols, and Mollisols, with a color value of five or lower, predominantly contained more aggregates, due to their relatively high clay content (e.g., Verisols) or high SOC content (e.g., Mollisol), and showed only half the spectral reflectance of the brighter soils. The spectrum, presented additionally in Figure 3, also shows the effect of averaging all of the 31 analyzed spectra according to the proportion of the area of these 11 soil great group units, which were the basis for calculating the $\alpha_{\theta s}$ distribution of soils representing all the bare soils in the arable land in Israel for any day of the year.

### *3.3. Half Diurnal Albedo Distribution*

Figure 4 presents examples of the half-diurnal ($\alpha_d$) distributions for these averaged soils, with roughness corresponding to the use of a Pd, an Hd, and an Hs, generated for chosen dates as a function of the solar local time. The averaged half-diurnal values of these soils, calculated for the shortest day of the year (22 December), were, respectively, 3.8%, 4.0%, and 4.8% higher than for the longest day (22 June). We were able to evaluate the accuracy of the predicted $a_{\theta_s}$ distributions using only the spectra of the Haploxeralfs, Rhodoxelalfs, and Xerothents, because only these three units had distributions also collected directly in the field. Figure 5 shows the measured and predicted $a_{\theta_s}$ distributions of the three additional units. $R^2$, calculated individually for these units up to 75° of $\theta_s$ at 1° increments, reached values higher than 0.92 for the Haploxeralfs and Xerothents, and only 0.87 for the Rhodoxeralf.

It was also found that the aggregated correctness of prediction for these three soils, expressed by the RMSE, was 0.025, and additionally, the plot of residuals of the prediction of $\alpha_{45}$ was generated to confirm that the residuals had a normal distribution (Figure 6). The residuals showed if the predicted value was higher or lower than the measured value, and in this case, they were roughly distributed symmetrically above and below the value of 0, meaning that model was not biased. The half-diurnal albedo of the soils formed by a Pd or an Hd was lower than that of the soils formed by an Hs of, respectively, about 45% and 25% at the beginning of the astronomical summer, compared to about 40% and 20% at the beginning of the astronomical winter (Figure 7a).

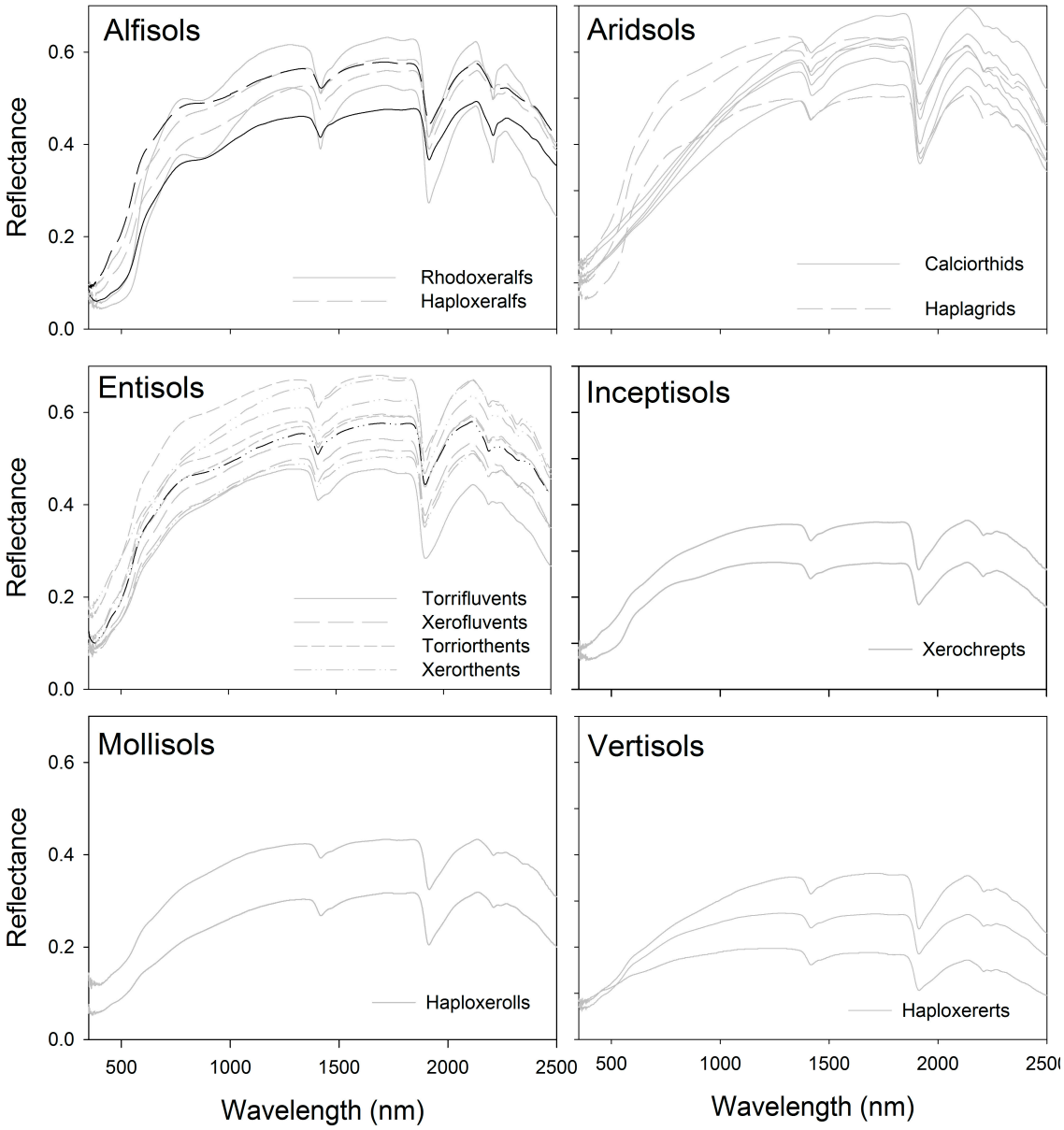


**Figure 3.** Reflectance spectra characterizing the analyzed soil units, obtained from ISDL (grey lines), analyzed in AMU (black lines), and the averaged spectrum describing all bare soil units within arable lands in Israel (bold black line).

### *3.4. Annual Distribution of Bare Soil*

The average annual distribution of the total bare soil area was described by a curve resembling an asymmetrical sinusoid, with its concave part being much narrower than its convex one (Figure 7b).

It was found that the minimum bare soil area occurred in winter, between the 30th and 60th day of the year (DOY) (in February), and the maximum appeared in summer until early autumn, between about 200th and 280th DOY (from the third decade of July to the first decade of October). It was found that this minimum and maximum reached about 500 and 2100 km$^2$, i.e., 13% and 55% of the arable land area in Israel, respectively.

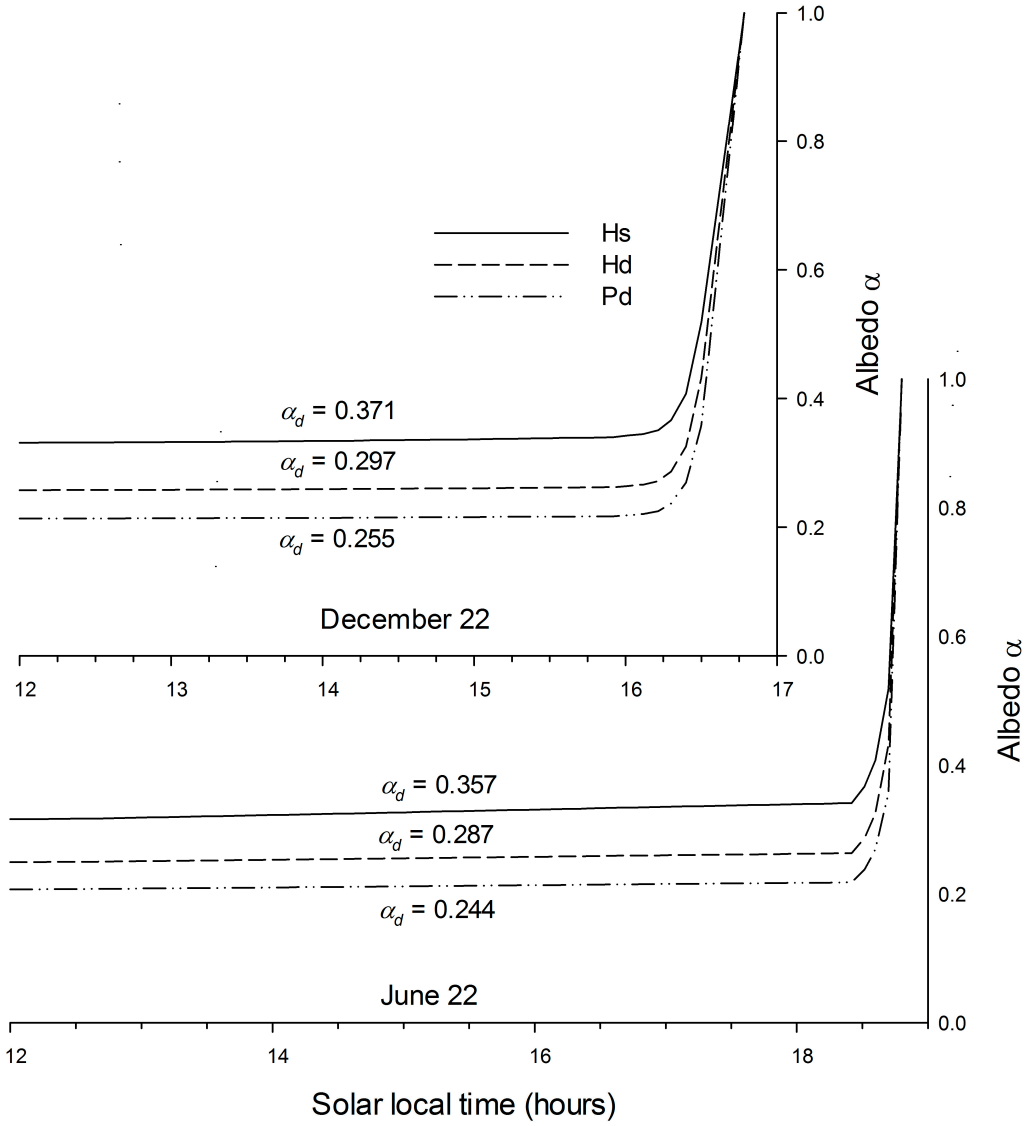


**Figure 4.** Half-diurnal albedo distributions of the average bare soils within arable lands in Israel, generated for the shortest (22 December) and the longest (22 June) day of the year, respectively, in relation to the local solar time.

### *3.5. Annual Incoming Radiation*

The total diurnal amount of shortwave radiation ($Ri_d$) reaching the analyzed soils in clear-sky conditions varied from about 14 TJ/km$^2$/day (at the beginning of the astronomical winter on the 356th DOY) to 31 TJ/km$^2$/day (at the beginning of the astronomical summer on the 172th DOY) (Figure 7c). The minimum of the amount of shortwave radiation that can be reflected from the averaged soils shaped by the analyzed farming tools ($Rrb_d$) were predicted at the turn of the year—between the 345th and 10th DOY (from the beginning of second decade of December to the end of the first decade of January) (Figure 7d). This minimum, occurring around the minimum $Ri_d$, was assessed at about

3.5 TJ/km$^2$/day, 4 TJ/km$^2$/d, and 5 TJ/km$^2$/day for the soils formed by a Pd, an Hd, and Hs, respectively. The maximum radiation was predicted in summer between the 150th and 200th DOY (from the beginning of June to the end of the second decade of July). The minimum and maximum values of $Rrb_d$ were expected around the extreme values of $Ri_d$.

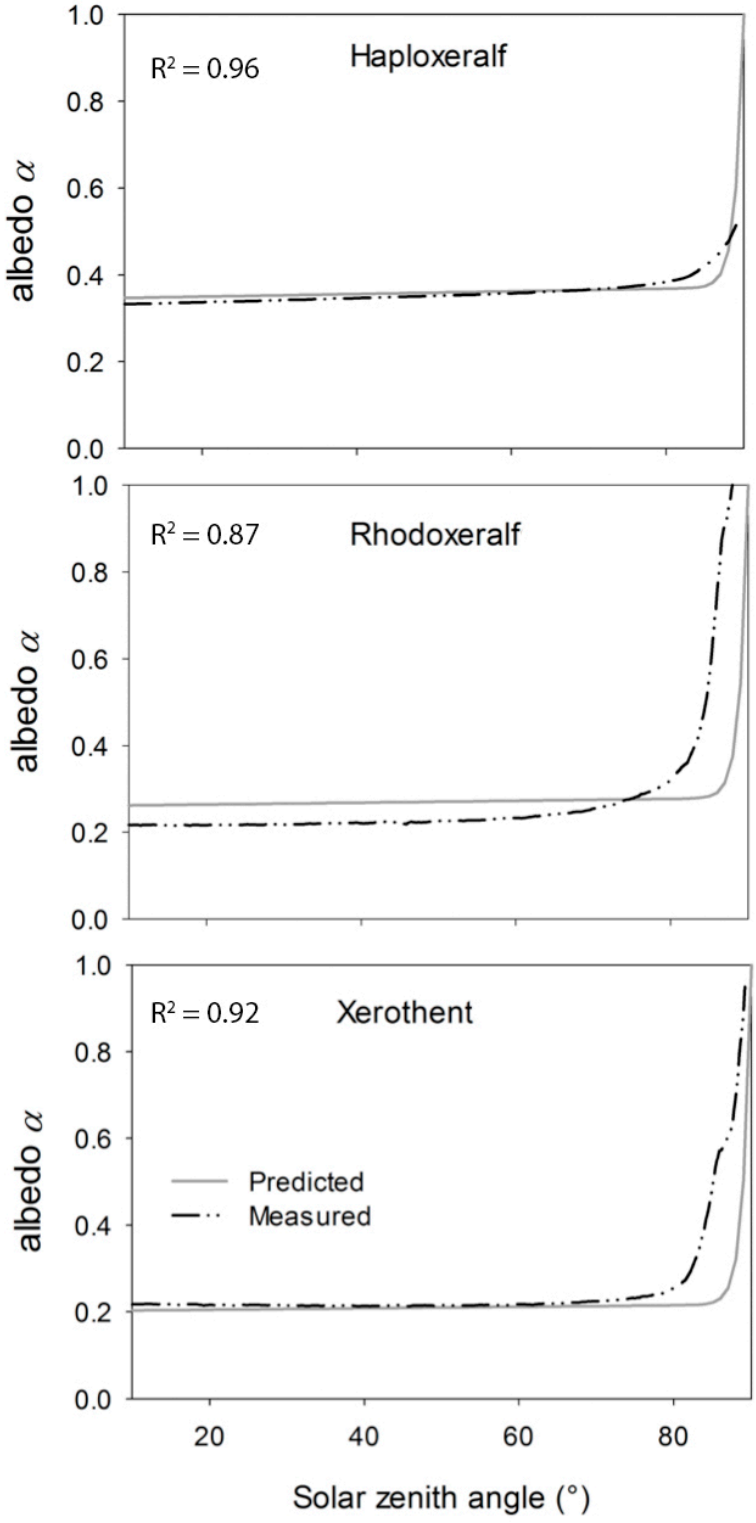


**Figure 5.** The half-diurnal albedo distributions of the Haploxeralfs, Rhodoxelalfs and Xerothents, measured and generated, for which their measurement data were directly collected in the field.

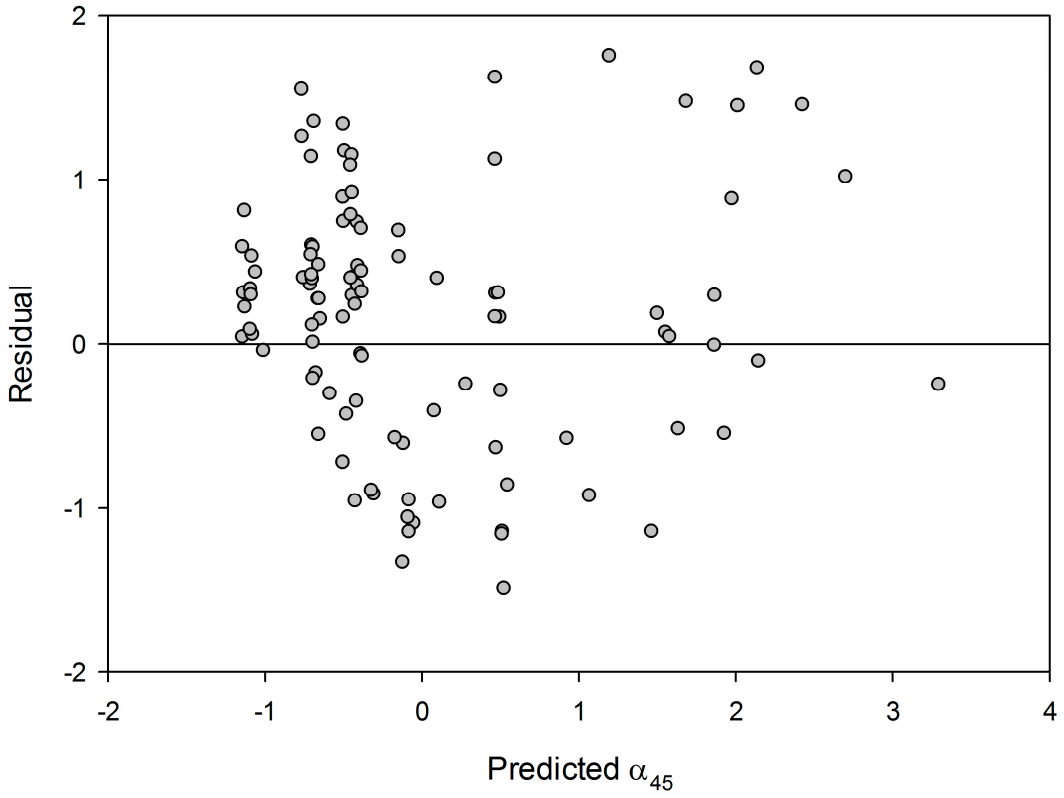


**Figure 6.** Plot of residuals showing normalized residuals versus normalized predicted values of $\alpha_{45}$.

### *3.6. Reflected Radiation Dependent on Roughness*

Without being able to distinguish bare soils formed by a Pd, an Hd, and an Hs individually from the analyzed Landsat images, and hence to estimate the proportion between thus-shaped areas of soils, it was only possible to determine the range of the total amount of shortwave radiation that could be reflected from the averaged bare soils on a given day of the year. This range in the annual course was defined between the total amount of reflected radiation, calculated for the soils formed by a Pd and an Hs, assuming that in both cases all these soils were treated only by one of these tools. Lower and upper values of this range were calculated, multiplying the $Rrb_d$ values related to the soils formed by a Pd and an Hs, respectively, by the total area of bare soils determined for a given DOY (Figure 7e). The minima, predicted in winter between the 1st and 70th DOY (from the beginning of January until the end of the first decade of March), were assessed at about 3 and 5 PJ/day for the lowest and the highest values of the range, respectively. Meanwhile, the maxima, expected in summer between about 200th and 250th DOY (from the beginning of the second decade of July to the end of the first decade of September), were assessed at about 16 and 23 PJ/day for the lowest and the highest values of the range. It was found that these extreme values occurred 40 days later than their equivalents, expressed as the amount of radiation reflected from one square kilometer of the soils shaped by a Pd and an Hs.

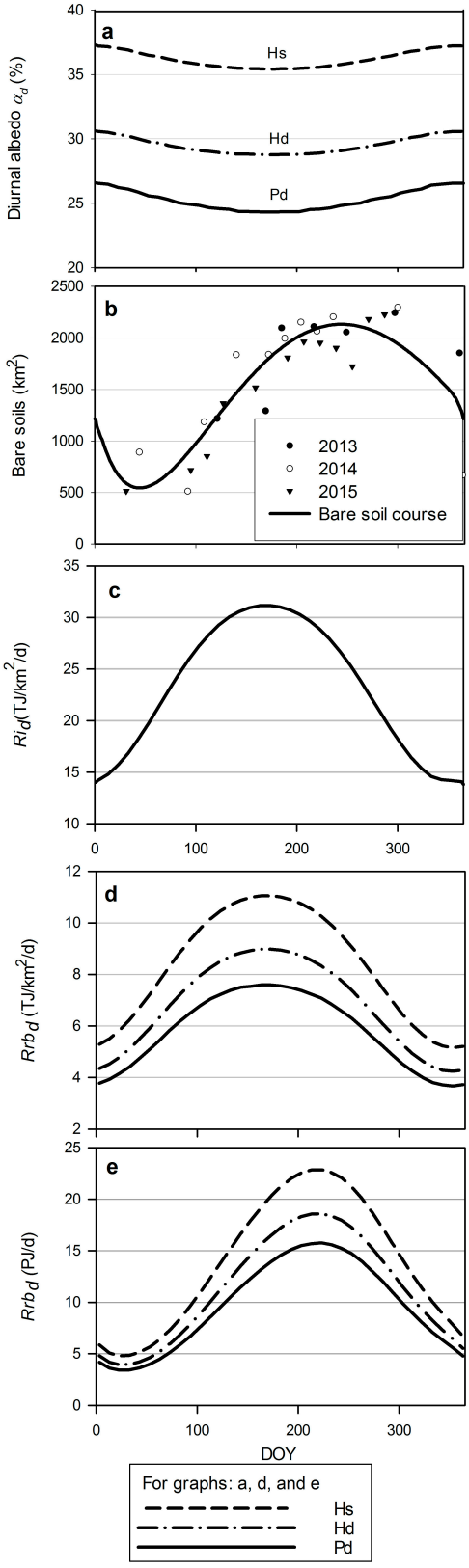


**Figure 7.** Annual variations in: (**a**) average diurnal albedo ($\alpha_d$) of the average bare soils within arable lands in Israel, formed by a plough (Pd), a disk harrow (Hd), and a smoothing harrow (Hs); (**b**) areas of bare soils within arable lands in Israel; (**c**) amount of shortwave radiation ($Ri_d$) reaching the soils in clear-sky conditions; (**d**) amount of shortwave radiation reflected from one square kilometer of the soils ($Rrb_d$); (**e**) amount of $Rrb_d$ reflected from all bare soils within arable lands in Israel. DOY—day of year.

## 4. Discussion

The study of the annual variation of shortwave radiation reflected from bare arable soil in clear-sky conditions has more real meaning in Israel than in Poland, where it was previously analyzed [21], particularly when comparing the multi-year average annual number of hours of sunshine in Israel versus Poland—about 3300 versus 1700, respectively (https://weather-and-climate.com/). It should also be noted that clear-sky conditions in the area studied in this research occurred most frequently during summer, on days when the discussed maximum of shortwave radiation of bare soils occurs. The area of arable land studied in this work is perhaps too small to effectively influence the climate on a global scale. The arable lands of Israel were very attractive for this research due to the high stability of sunny days, making it very useful for collecting the half-diurnal albedo of soils in various roughness states, as well as due to the different distributions of the radiation maximum in Israel compared to Poland.

The quantitative estimation of the amount of shortwave radiation that could be reflected by bare cultivated soils requires further studies of arable lands over larger areas. In the future, by using tools that enable us to quantify the annual variation in shortwave radiation reaching the studied soils and collecting data characterizing the variation of their surface moisture, the issue presented today under limited conditions could be described in a more comprehensive way.

Investigating how strongly the amount of shortwave radiation reflected from bare soils (depending on their roughness, as presented in this paper) affects their amount of emitted long-wave radiation could help us more closely and accurately assess the impact of agricultural practices on the climate on a regional and global scale [28,29].

## 5. Concluding Remarks

The results obtained in this study show a clear annual variation of the amount of short-wave radiation reflected from all bare soils within arable land in Israel. It was assessed that the winter minimum radiation (occurring between the 1st and 70th DOY) and the summer maximum radiation (predicted between 200th and 250th DOY) could reach about 3–5 PJ/day and 16–23 PJ/day from one square kilometer of soil, respectively. The lower values of these ranges relate to the soils formed by a plow, and the higher ones a smoothing harrow.

The quantitative dependence between soil surface properties and the diurnal variation of broadband blue-sky albedo requires further studies of arable lands over larger areas, possibly including thermal channel data. We do not have sufficient competence to assess whether the amount of the predicted radiation could have a noticeable impact on the climate on a regional or global scale and doubtless these results need to be considered by climatologists.

**Acknowledgments:** This work was supported by the Polish National Science Centre within the framework of project no. 2014/13/B/ST10/02111.

**Author Contributions:** Jerzy Cierniewski conceived the idea and wrote most of the paper, Jakub Ceglarek performed the field experiments and, together with Sławomir Królewicz and Cezary Kaźmierowski, analyzed the data. Arnon Karnieli arranged and facilitated field experiments in Israel and Eyal Ben-Dor provided soil spectral data.

**Conflicts of Interest:** The authors declare no conflicts of interest.

## References

1. Dobos, E. Albedo. In *Encyclopedia of Soil Science*; Taylor & Francis: London, UK, 2006.
2. Oke, T.R. *Boundary Layer Climates*; Routledge: London, UK, 1992.
3. Rechid, D.; Jacob, D.; Hagemann, S.; Raddatz, T.J. Vegetation effect on land surface albedo: Method to separate vegetation albedo from the underlying surface using satellite data. *Geophys. Res. Abstr.* **2005**, *7*, 7962.
4. Baumgardner, M.; Silva, L.; Biehl, L.; Stoner, E. Reflectance properties of soils. *Adv. Agron.* **1986**, *38*, 1–44.
5. Cipra, J.E.; Baumgardner, M.F.; Stoner, E.R.; MacDonald, R.B. Measuring Radiance Characteristics of Soil with a Field Spectroradiometer1. *Soil Sci. Soc. Am. J.* **1971**, *35*, 1014. [CrossRef]

6. Goldshleger, N.; Ben-Dor, E.; Benyamini, Y.; Agassi, M. Soil reflectance as a tool for assessing physical crust arrangement of four typical soils in israel. *Soil Sci.* **2005**, *169*, 677–687. [CrossRef]
7. Mikhajlova, N.A.; Orlov, D.S. *Opticheskie Svoystva Pochv i Pochvennych Komponentov*; Russ. Nauka: Moscow, Russia, 1986.
8. Matthias, A.D.D.; Fimbres, A.; Sano, E.E.E.; Post, D.F.F.; Accioly, L.; Batchily, A.K.K.; Ferreira, L.G.G. Surface roughness effects on soil albedo. *Soil Sci. Soc. Am. J.* **2000**, *64*, 1035–1041. [CrossRef]
9. Ben-Gai, T.; Bitan, A.; Manes, A.; Alpert, P.; Rubin, S. Spatial and Temporal Changes in Rainfall Frequency Distribution Patterns in Israel. *Theor. Appl. Climatol.* **1998**, *61*, 177–190. [CrossRef]
10. Schneider, S.H.; Dickinson, R.E. Climate modeling. *Rev. Geophys.* **1974**, *12*, 447. [CrossRef]
11. Davin, E.L.; de Noblet-Ducoudré, N.; Friedlingstein, P. Impact of land cover change on surface climate: Relevance of the radiative forcing concept. *Geophys. Res. Lett.* **2007**, *34*. [CrossRef]
12. Monteith, J.L.; Szeicz, G. The radiation balance of bare soil and vegetation. *Q. J. R. Meteorol. Soc.* **1961**, *87*, 159–170. [CrossRef]
13. Lewis, P.; Barnsley, M.J. Influence of the Sky Radiance Distribution on Various Formulations of the Earth Surface Albedo. In Proceedings of the 6th International Symposium on Physical Measurements and Signatures in Remote Sensing, Val d'Isere, France, 17–21 January 1994; pp. 707–716.
14. Wang, K.; Wang, P.; Liu, J.; Sparrow, M.; Haginoya, S.; Zhou, X. Variation of surface albedo and soil thermal parameters with soil moisture content at a semi-desert site on the western Tibetan Plateau. *Bound. Layer Meteorol.* **2005**, *116*, 117–129. [CrossRef]
15. Oguntunde, P.G.; Ajayi, A.E.; Giesen, N. van de Tillage and surface moisture effects on bare-soil albedo of a tropical loamy sand. *Soil Tillage Res.* **2006**, *85*, 107–114. [CrossRef]
16. Cierniewski, J.; Karnieli, A.; Kazmierowski, C.; Krolewicz, S.; Piekarczyk, J.; Lewinska, K.; Goldberg, A.; Wesolowski, R.; Orzechowski, M.; Kaźmierowski, C.; et al. Effects of soil surface irregularities on the diurnal variation of soil broadband blue-sky albedo. *IEEE J. Sel. Top. Appl. Earth Obs. Remote Sens.* **2015**, *8*, 493–502. [CrossRef]
17. Sellers, P.J.; Meeson, B.W.; Hall, F.G.; Asrar, G.; Murphy, R.E.; Schiffer, R.A.; Bretherton, F.P.; Dickinson, R.E.; Ellingson, R.G.; Field, C.B.; et al. Remote sensing of the land surface for studies of global change: Models—Algorithms—Experiments. *Remote Sens. Environ.* **1995**, *51*, 3–26. [CrossRef]
18. Grant, I.F.; Prata, A.J.; Cechet, R.P. The Impact of the Diurnal Variation of Albedo on the Remote Sensing of the Daily Mean Albedo of Grassland. *J. Appl. Meteorol.* **2000**, *39*, 231–244. [CrossRef]
19. Cierniewski, J.; Kazmierowski, C.; Krolewicz, S.; Piekarczyk, J. Effects of soil roughness on the optimal time of cultivated soils observation by satellites for the soils average diurnal albedo approximation. *IEEE J. Sel. Top. Appl. Earth Obs. Remote Sens.* **2013**, *6*, 1194–1198. [CrossRef]
20. Cierniewski, J.; Krolewicz, S.; Kazmierowski, C.; Ceglarek, J.; Kusz, P. Shortwave radiation reflected from the territory of Poland throughout the year as an effect of smoothing soils previously plowed and harrowed. In Proceedings of the IEEE International Geoscience and Remote Sensing Symposium (IGARSS), Milan, Italy, 26–31 July 2015; pp. 4629–4632.
21. Cierniewski, J.; Królewicz, S.; Kaźmierowski, C. Annual dynamics of shortwave radiation as consequence of smoothing of previously plowed and harrowed soils in Poland. *J. Appl. Meteorol. Climatol.* **2017**, *56*, 735–743. [CrossRef]
22. Richter, R.; Schlapfer, D. Atmospheric/Topographic Correction for Satellite Imagery-ATCOR2/3 User Guide. Available online: http://www.rese.ch/pdf/atcor3_manual.pdf (accessed on 9 March 2018).
23. Ravikovitch, S. *Guidebook and Map of Israel Soils*; Hebrew University Magnes Press: Jerusalem, Israel, 1969.
24. Soil Survey Staff Soil Survey Field and Laboratory Methods Manual. *Soil Survey Investigations Report No. 51, Version 2.0*; U.S. Department of Agriculture: Lincoln, Nebraska, 2014; p. 407.
25. Cierniewski, J.; Ceglarek, J.; Karnieli, A.; Krolewicz, S.; Kazmierowski, C.; Zagajewski, B. Predicting the diurnal blue-sky albedo of soils using their laboratory reflectance spectra and roughness indices. *J. Quant. Spectrosc. Radiat. Trans.* **2017**, *200*, 25–31. [CrossRef]
26. Taconet, O.; Ciarletti, V. Estimating soil roughness indices on a ridge-and-furrow surface using stereo photogrammetry. *Soil Tillage Res.* **2007**, *93*, 64–76. [CrossRef]
27. Allen, R.G.; Rick, G.; Food and Agriculture Organization of the United Nations. *Crop Evapotranspiration: Guidelines for Computing Crop Water Requirements*; Food and Agriculture Organization of the United Nations: Rome, Italy, 1998; ISBN 9251042195.

28. Kustas, W.P.; Norman, J.M. Use of remote sensing for evapotranspiration monitoring over land surfaces. *Hydrol. Sci. J.* **1996**, *41*, 495–516. [CrossRef]
29. Mira, M.; Olioso, A.; Gallego-Elvira, B.; Courault, D.; Garrigues, S.; Marloie, O.; Hagolle, O.; Guillevic, P.; Boulet, G. Uncertainty assessment of surface net radiation derived from Landsat images. *Remote Sens. Environ.* **2016**, *175*, 251–270. [CrossRef]